405 Trabecular Meshwork, Ciliary Body and Anterior Segment Imaging
Wednesday, May 10, 2017 8:30 AM–10:15 AM
Ballroom 4 Paper Session
Program #/Board # Range: 3768–3774
Organizing Section: Glaucoma

Program Number: 3768
Presentation Time: 8:30 AM–8:45 AM
Predicting the Outcome of Laser Peripheral Iridotomy for Primary Angle Closure Suspect Eyes using Anterior Segment Optical Coherence Tomography
Victor T. Koh[1], Muhammad Reza Keshtkaran[2], Paul T. Chew[1], Maria Cecilia D. Aquino[1], Chelvin Sng[1]. [1]Ophthalmology, National University Hospital, Singapore, Singapore; [2]Ophthalmology, National University of Singapore, Singapore, Singapore.
Purpose: To develop an automated algorithm to predict the success probability of laser peripheral iridotomy (LPI) in eyes with primary angle closure suspect (PACS), using anterior chamber angle (ACA) characteristics of pre-treatment anterior segment optical coherence tomography (AS-OCT) scans.
Methods: A total of 76 eyes with PACS underwent LPI and time-domain AS-OCT scans (temporal and nasal cuts) were performed before and 1 month after LPI. All the post-treatment scans were graded by a trained ophthalmologist to one of the following categories: (a) both angles open, (b) one of two angles open and (c) both angles closed. After LPI, success is defined as one or more angles changed from close to open on the AS-OCT images. Only AS-OCT scans with sufficient quality and if the scleral spur can be identified were selected for analysis. All the pre-treatment ASOCT scans were analyzed using the Anterior Segment Analysis Program to derive 76 ACA measurements which serve as features for a subsequent prediction algorithm.
Results: In total, we included 76 eyes and 50 (65.8%) eyes fulfilled the criteria for success after LPI. Among the 76 ACA features, three features including iris thickness at the dilator muscle region [measured at half of the distance between the scleral spur and the pupillary margin], iris thickness measured at 2000 um from the scleral spur and trabecular iris space area (TISA 500) had the highest predictive score and they were selected using correlation-based subset selection method. These features were classified into two ('successful' and 'unsuccessful') categories using a Bayes classifier. The success of LPI in eyes with narrow angles can be predicted with 77.9% cross validation accuracy.
Conclusions: Our study showed that using pre-treatment AS-OCT scans, an automated algorithm can show reasonable accuracy in predicting the success of LPI in improving ACA parameters in PACS eyes. Further analysis using newer AS-OCT parameters and algorithm could potentially guide ophthalmologists in deciding when to offer LPI as a prophylaxis for PACS
Commercial Relationships: Victor T. Koh, None; **Muhammad Reza Keshtkaran**, None; **Paul T. Chew**, None; **Maria Cecilia D. Aquino**, None; **Chelvin Sng**, None

Program Number: 3769
Presentation Time: 8:45 AM–9:00 AM
Non-invasive in vivo mapping of aqueous outflow and lymphatic drainage from the eye
Kirsten Cardinell[1], Yeni H. Yucel[1, 2], Xun Zhou[1], Neeru Gupta[1, 2]. [1]Keenan Research Centre for Biomedical Science, St. Michael's Hospital, Toronto, ON, Canada; [2]Departments of Laboratory Medicine and Pathobiology, and Ophthalmology and Vision Sciences, University of Toronto, Toronto, ON, Canada.
Purpose: The purpose of this study is to non-invasively map aqueous outflow and lymphatic drainage from the eye in vivo.
Methods: Tracer dye called QC-1 absorbs light in the near infrared range, and was used to track aqueous humour movement. Photoacoustic tomography (PAT), a light and sound based imaging technology, was used to track QC-1 in vivo. For in vitro imaging, agar phantoms were generated using 10 serial dilutions of QC-1. For in vivo imaging, 0.5μL Bovine Serum Albumin (10mg/mL; Sigma-Aldrich, USA) conjugated with IRDye QC-1 (LI-COR, USA) was injected intracamerally into the right eye of 9 CD-1 mice under general anesthesia. Mice were scanned using PAT (MSOT inVision 128, iThera Medical, Germany). Cross-sectional imaging of the head and neck (150 μm; 0.5 mm steps) at wavelengths from 680 to 900 nm before and 10 min, 1 hr, 2 hrs, 4 hrs, and 6 hrs after injection. MSOT software was used to reconstruct and detect QC-1 signal. The mean pixel intensity was measured in both eyes and cervical lymph nodes. The slope of change in normalized mean pixel intensity from 10 min to 6 hrs was calculated for each region of interest. The difference in slopes at 2.5 hrs between eyes (n=9) was compared using t-test. A similar analysis was performed for in 4 mice with detectable signal in nodes.
Results: Phantoms showed a linear relationship between QC-1 dye concentration and photoacoustic signal. Strong QC-1 signal was detected in the right eye of all mice (n=9) (Fig1A). Decreasing QC-1 signal was observed at 1 h, 2 hrs, 4 hrs and 6 hrs (Fig1B). QC-1 signal in right cervical nodes was seen at 2 hrs after injection with a peak at 4 hrs (n=4)(Fig1C). No QC-1 signal was detected in the left eye and left cervical nodes. Slope differences at 2.5 hr between right and left eyes was significant (n=9; $P<0.01$), as was the difference between right and left nodes (n=4; $P= 0.01$).
Conclusions: This is the first study to assess outflow and lymphatic drainage in vivo in the infrared range. Further studies to quantify the photoacoustic signal will help to understand outflow in the normal eye and in response to glaucoma drugs.
Acknowledgments: CIHR, CFI, Henry Farrugia and Nicky & Thor Eaton Research Funds.

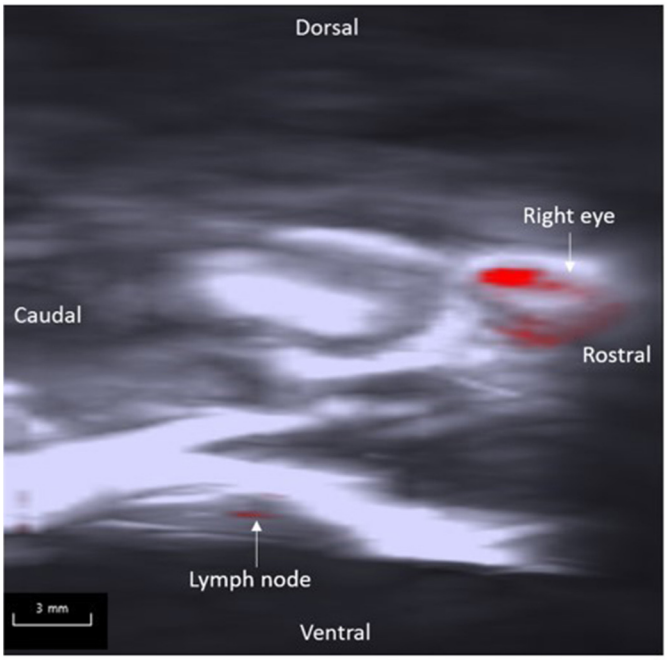

Fig 1

Fig 1 2 hrs after intracameral injection, QC-1 signal is seen in the right eye and cervical node.

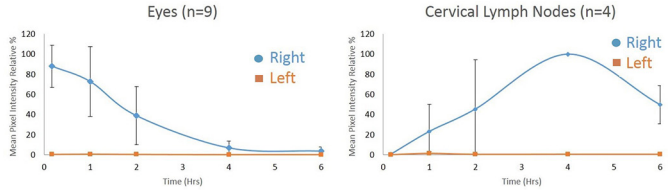

Fig 2A Fig 2B

Fig 2A and Fig 2B show QC-1 signal intensity in eyes (n=9) and nodes (n=4) over time.

Commercial Relationships: Kirsten Cardinell; **Yeni H. Yucel**, None; **Xun Zhou**, None; **Neeru Gupta**, None

Support: CIHR (MOP119432), CFI (31326), Henry Farrugia and Nicky & Thor Eaton Research Funds.

Program Number: 3770

Presentation Time: 9:00 AM–9:15 AM

Aqueous Angiography: Real-time, Live Human and Non-Human Primate Aqueous Humor Outflow Imaging

Alex S. Huang[1, 2], Meng Li[5, 6], Diya Yang[5, 6], Ben Xu[3], Andrew Camp[3, 4], huaizhou wang[5, 6], Ningli Wang[5, 6], Robert N. Weinreb[3, 4].

[1]Ophthalmology, Doheny Eye Institute, Los Angeles, CA; [2]University of California, Los Angeles, Los Angeles, CA; [3]University of California, San Diego, La Jolla, CA; [4]Shiley Eye Institute, San Diego, CA; [5]Ophthalmology, Beijing Tongren Hospital, Beijing, China; [6]Capital Medical University, Beijing, China.

Purpose: To evaluate aqueous humor outflow (AHO) in intact eyes of living humans and non-human primates (NHP) using aqueous angiography

Methods: Aqueous angiography was performed for the first time in intact eyes of living subjects (6 NHP and one living human [73 yo male during cataract surgery]). After anesthesia, an anterior chamber (AC) maintainer was placed through a temporal 1 mm side-port wound. Indocyanine green (ICG; 0.4%) or 2.5% fluorescein was introduced (individually or in sequence) into the eye with a gravity-driven constant-pressure system. Aqueous angiography images were obtained with a Heidelberg Spectralis HRA+OCT suspended over the eye using a custom designed surgical boom arm (FLEX module). For NHPs, anterior segment optical coherence tomography (OCT) images were taken comparing angiographically positive and negative regions.

Results: In NHP, aqueous angiography positive signal co-localized with episcleral veins as identified by infrared imaging (Fig. 1). Areas with aqueous angiography signal also showed intrascleral lumens using anterior segment OCT. Sequential aqueous angiography in individual eyes with ICG followed by fluorescein showed similar, segmental, and mostly stable patterns. A pulsatile nature of angiographic AHO was sometimes seen. Aqueous angiographic patterns could also sometimes dynamically change. In some cases, regions without aqueous angiography signal could develop signal. Alternatively, angiographic signal could also suddenly disappear from regions in which angiographic signal was initially documented. In the living human subject, aqueous angiography was successfully performed with demonstrating segmental patterns with no adverse sequelae

Conclusions: Aqueous angiography was conducted for the first time in intact eyes of living NHPs and one human subject demonstrating segmental and pulsatile patterns. The ability for angiographic AHO patterns to dynamically shift and move in the intact eye of a living NHP was a new discovery. Real-time imaging of AHO improves our understanding of the eye and may have surgical glaucoma treatment implications.

Figure 1
Huang et al

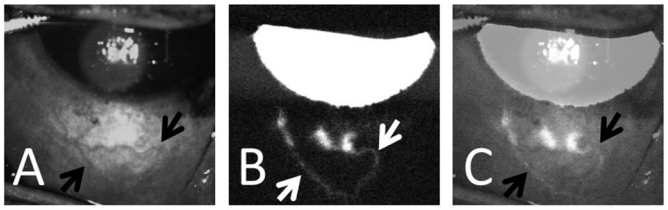

Figure 1. A) Infrared reflectance image of a NHP right eye shows episcleral veins (black arrows). B) Aqueous Angiography signal from the same eye (white arrows). C) Image overlap shows good correspondence between aqueous angiography signal and episcleral veins.

Commercial Relationships: Alex S. Huang, Heidelberg Engineering (F), Allergan (C); **Meng Li**, None; **Diya Yang**, None; **Ben Xu**, None; **Andrew Camp**, None; **huaizhou wang**, None; **Ningli Wang**, None; **Robert N. Weinreb**, Heidelberg Engineering (F), Aerie Pharmaceutical (C), Alcon (C), Carl Zeiss Meditec (F), Quark (F), Forsight Vision V Sensimed (C), Topcon (F), Optovue (F), Eyenovia (C), Bausch & Lomb (C), Genentech (F), Allergan (C), Unity (C)

Support: Supported by National Institutes of Health, Bethesda, Maryland (K08EY024674 [ASH]); Research to Prevent Blindness Career Development Award 2016 [ASH]; and an unrestricted grant from Research to Prevent Blindness (New York, NY).

Program Number: 3771
Presentation Time: 9:15 AM–9:30 AM
Contractile features of the distal aqueous drainage tract
James C. Tan[1], Jose Gonzalez[1], MinHee K. Ko[1], Andrius Masedunskas[2], Roberto Weigert[3], Young Hong[4]. [1]UCLA Department of Ophthalmology, Doheny Eye Institute, Pasadena, CA; [2]School of Medical Sciences, University of New South Wales, Kensington, NSW, Australia; [3]National Cancer Institute, National Institutes of Health, Bethesda, MD; [4]Surgery, University of Southern California Keck School of Medicine, Los Angeles, CA.
Purpose: Outflow resistance in the aqueous drainage tract distal to trabecular meshwork (TM) is potentially an important determinant of intraocular pressure (IOP). It may also influence the success of treatments and surgeries directing aqueous into the distal system. Mechanisms controlling distal resistance are unclear. We hypothesize that contractility is a mechanism influencing aqueous vessel caliber and resistance in analogous fashion to its role in controlling blood vessel tone.
Methods: We determined if cells with a smooth muscle identity populate the distal aqueous vessel walls. 2-photon imaging was performed of live and postmortem mouse eyes. Transgenic reporter mice expressing a fluorescent endothelial marker (Prox1) and wild-type control mice were studied as models of the human system. Hoechst 33342-nuclear staining and F-actin labeling with fluorescence-conjugated phalloidin were used to characterize the cellularity of the cells lining aqueous vessels.
Results: We imaged deep in the sclera to identify distal aqueous vessels. Aqueous vessels appeared as second harmonic generation signal voids amongst the scleral collagen fibers. Vessels and their cells were tracked from episcleral veins to their origins in Schlemm's Canal. The Prox1 reporter revealed that endothelium was present in the outer wall of Schlemm's Canal, collector channels and the proximal regions of aqueous vessels. Two distinct cells layers were identified surrounding the lumen of aqueous vessels: (1) endothelium immediately bordered the lumen of aqueous vessels and (2) external to endothelium were cells in a contracted state that expressed smooth muscle markers (eg., alpha smooth muscle actin) in a profile similar to that of arterial walls and ciliary muscle.
Conclusions: Our findings support an organization of aqueous vessel walls resembling that of blood vessels. A central lumen lined by endothelium is surrounded by cells with contractile features bearing a smooth muscle identity. This reflects a capacity to contract and could support dynamic alteration of aqueous vessel caliber and resistance analogous to the role of vascular tone in regulating blood flow.
Commercial Relationships: James C. Tan, None; **Jose Gonzalez**, None; **MinHee K. Ko**, None; **Andrius Masedunskas**, None; **Roberto Weigert**, None; **Young Hong**, None
Support: NIH Grant EY020863 (JCHT), EY03040 (Doheny Vision Research Institute Imaging Core), Kirchgessner Foundation Research Grant (JCHT), American Glaucoma Society Mentoring for Physician Scientists Award and Young Clinician Scientist Award (JCHT), Career Development Award from Research to Prevent Blindness (JCHT), and an unrestricted grant from the Research to Prevent Blindness, Inc., New York, NY.

Program Number: 3772
Presentation Time: 9:30 AM–9:45 AM
Role of Primary Cilia in Trabecular Meshwork Cell Function
Ankur Jain[1], Wei Zhu[2], Qihong Zhang[1], Markus H. Kuehn[2], Abbot F. Clark[3], Val Sheffield[1]. [1]Pediatrics, University of Iowa, Iowa City, IA; [2]Ophthalmology, University of Iowa, Iowa City, IA; [3]Cell Biology and Immunology, UNT Health Science Center, Fort Worth, TX.
Purpose: Intraocular pressure (IOP) is mostly regulated by aqueous humor outflow through the trabecular meshwork (TM) and represents the only modifiable risk factor for glaucoma. Primary cilia are specialized organelles that play an important role in intraflagellar transport. The importance of primary cilia is observed in a group of disorders termed "ciliopathies". The mechano-sensing role of primary cilia in TM function, IOP regulation and glaucoma remains largely unknown.
Methods: Number of cilia positive cells and ciliary lengths (immunochemically using anti-ARL13b antibody) were compared among cultured human primary normal (NTM) and glaucomatous TM (GTM) cell strains and tissues (n=3). Cilia were targeted by both chemical agents such as chloral hydrate and sodium pyrophosphate, and siRNA and CRISPR/Cas9 against intraflagellar proteins to study the effects on glaucoma-related insults including dexamethasone (DEX) and TGFβ2 signaling in TM.
Results: Cultured GTM cell strains appear to have longer primary cilia as compared to NTM. Disrupting cilia results in affected DEX and TGFβ2 signaling (measured by SMAD and GRE-promoter reporter assays) as well as extracellular matrix synthesis in TM.
Conclusions: The differences among primary cilia on GTM vs NTM cell strains and involvement of primary cilia in DEX and TGFβ2 signaling suggest a prominent role of primary cilia in TM function and potential involvement in glaucoma pathophysiology.
Commercial Relationships: Ankur Jain; **Wei Zhu**, None; **Qihong Zhang**, None; **Markus H. Kuehn**, None; **Abbot F. Clark**, None; **Val Sheffield**, None

Program Number: 3773
Presentation Time: 9:45 AM–10:00 AM
Stretch-Dependent Pore Formation in Glaucomatous Schlemm's Canal Cells
Darryl R. Overby[1], Sietse Braakman[1], Alice Spenlehauer[1], Justino R. Rodrigues[1], Carter Teal[1], A T. Read[2], W Daniel Stamer[3], C R. Ethier[2]. [1]Department of Bioengineering, Imperial College London, London, United Kingdom; [2]Wallace H. Coulter Department of Biomedical Engineering, Georgia Institute of Technology & Emory University School of Medicine, Atlanta, GA; [3]Duke Eye Center, Duke University School of Medicine, Durham, NC.
Purpose: Micron-sized pores provide a pathway for aqueous humor drainage across Schlemm's canal (SC) endothelium. SC pore density is reduced in glaucoma, and glaucomatous SC cells have impaired pore-forming ability compared to normal SC cells exposed to the same transendothelial pressure drop (Overby et al., *PNAS* 2014). In this study, we compare pore density between normal and glaucomatous SC cells exposed to the same levels of mechanical stretch. Imposing stretch (vs. imposing transendothelial pressure drop) minimizes the influence of cellular stiffness that correlates with pore density in pressure-controlled experiments.
Methods: Human SC cells were isolated from 1 glaucomatous (SC57g) and 1 non-glaucomatous donor (SC67) and characterized by established protocols (Perkumas and Stamer, *EER* 2012). SC cells were seeded at $24x10^3$ cells/cm^2 on elastic PDMS membranes coated with biotinylated gelatin. Once confluent, cells were exposed to 0%, 10% or 20% equibiaxial stretch (N=2-4 samples each), incubated with FITC-avidin tracer for 3 minutes and then fixed at 6 minutes post-stretch. We identified pores based on accumulation of tracer where it crossed the SC monolayer and bound to the PDMS membrane, following Dubrovskyi et al. (*Lab Invest* 2013) and Braakman et al. (ARVO 2014). We focused on transcellular 'I' pores, identified as circular tracer spots underneath individual cells away from cell borders. Tracer patterns were imaged at 20x by epifluorescence microscopy covering 3 mm^2 (15-20 non-overlapping

images) per sample. One masked observer (STB) identified and counted I-pores. Pore density was analyzed using Poisson statistics.
Results: At 0% stretch, I-pore density was similar between SC67 (41±17 pores/mm^2; mean±SD) and SC57g (47±19 pores/mm^2). Pore density increased with stretch in SC67 ($p<10^{-5}$) and SC57g ($p<0.03$; Figure). However, the linear slope of pore density versus stretch was significantly lower in SC57g versus SC67 ($p<0.003$; ANCOVA).
Conclusions: Transcellular pore formation was reduced in glaucomatous relative to normal SC cells when controlling for mechanical stretch. This suggests a deficiency in the biomolecular machinery responsible for I-pore formation in glaucomatous SC cells that is maintained in culture. Ongoing studies will compare tracer-based pore detection against scanning electron microscopy.

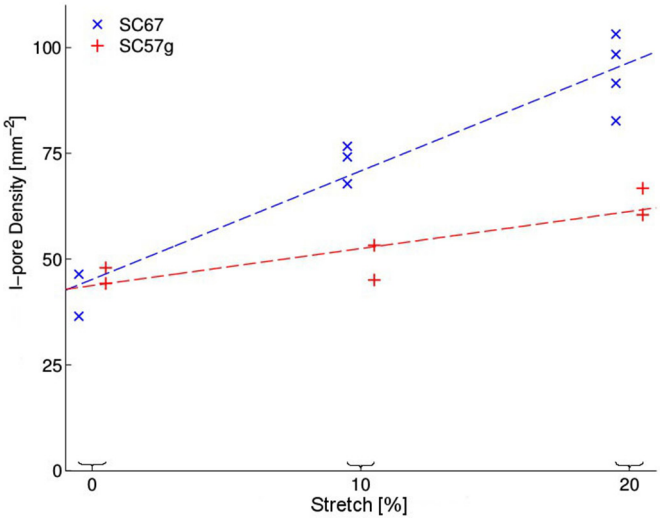

Tracer-based measurements of I-pore density as a function of stretch in normal (SC67) and glaucomatous (SC57g) SC cells.
Commercial Relationships: Darryl R. Overby; **Sietse Braakman**, None; **Alice Spenlehauer**, None; **Justino R. Rodrigues**, None; **Carter Teal**, None; **A T. Read**, None; **W Daniel Stamer**, None; **C R. Ethier**, None
Support: NIH Grant EY019696 and the Georgia Research Alliance

Program Number: 3774
Presentation Time: 10:00 AM–10:15 AM
Transplantation of iPSC-TM decreases IOP in aged sGC$^{-/-}$ mice
Wei Zhu[1, 2], Emmanuel S. Buys[3], Markus H. Kuehn[2, 4]. [1]Pharmacology Department, Qingdao University, Qingdao, China; [2]Department of Ophthalmology and Visual Sciences, the University of Iowa, Iowa City, IA; [3]Department of Anesthesia, Massachusetts General Hospital Research Institute, Boston, MA; [4]Veterans Affairs Medical Center, Center for the prevention and treatment of visual loss, Iowa City, IA.

Purpose: We previously investigated the therapeutic role of induced pluripotent stem cells derived trabecular meshwork cells (iPSC-TM) in glaucomatous myocilin^{Y437H} transgenic mice. The goal of this study was to test the effect of iPSC-TM in a distinct glaucomatous mouse model caused by the deficiency of soluble guanylate cyclase (sGC) and to determine the therapeutic potential of iPSC-TM transplantation in aged mice.
Methods: TM cellularity in 14-mon-old sGC$^{-/-}$ mice (n=6) and age matched WT mice (n=8) was assessed by immunohistochemistry (IHC). iPSC-TM were purified and characterized by IHC. 50,000 iPSC-TM were injected into the anterior chamber of 12 month-old sGC$^{-/-}$ mice (n=15). Age matched PBS recipients (n=7) and wild type mice (n=8) were used as the vehicle and positive control. IOP was tracked by rebound tonometry. TM cellularity after transplantation was analyzed using morphometric approaches.
Results: TM cellularity was lower in 14-month-old sGC$^{-/-}$ mice than in age matched WT mice (17.78 and 24.97 TM cells/section, respectivelyP=0.046). Four weeks after injection of iPSC-TM or an equal volume PBS (vehicle control) into the anterior chamber of 12-month-old sGC$^{-/-}$ mice, IOP was still similar in iPSC-TM recipients and vehicle control mice (13.98 mmHg and 14.42 mmHg, respectively P=0.60) and higher than in age-matched WT mice (11.60 mmHg). However, seven weeks after treatment, IOP was lower in iPSC-TM recipients than in vehicle control mice (12.71 mmHg and 13.78 mmHg, respectively, P=0.046). The IOP measured in transplanted mice is similar to that of WT mice (12.97 mmHg). Morphometric analysis revealed higher TM cellularity in iPSC-TM recipients than in vehicle control mice (22.34 and 16.42 TM cells/anterior segment, respectively, P=0.0059). TM cellularity was similar in iPSC-TM recipients and WT mice (24.9 TM cells/anterior segment).
Conclusions: Restoration of the TM via iPSC-TM transplantation is an efficient approach to treat TM degeneration resulting from a variety of etiologies. Furthermore, transplantation improves IOP and TM cellularity even in very old individuals. These are encouraging findings indicating the therapeutic potential of regenerating the TM in the majority of POAG cases.
Commercial Relationships: Wei Zhu, None; **Emmanuel S. Buys**, None; **Markus H. Kuehn**, None